Attitude and Altitude Tracking Controller for Quadcopter Dynamical Systems

MANAL S. ESMAIL[1,2]**, MOHAMED H. MERZBAN**[3]**, ASHRAF A. M. KHALAF**[2]**,
HESHAM F. A. HAMED**[2,4]**, AND AZIZA I. HUSSEIN**[5]**, (Member, IEEE)**

[1]Department of Electrical Engineering, Future High Institute of Engineering, Dimu, Fayoum 63511, Egypt
[2]Department of Electrical Engineering, Faculty of Engineering, Minia University, Minia 61519, Egypt
[3]Department of Electrical Engineering, Faculty of Engineering, Fayoum University, Faiyum 63511, Egypt
[4]Department of Telecommunication, Faculty of Engineering, Egyptian Russian University, Cairo, Badr City 11829, Egypt
[5]Department of Electrical and Computer Engineering, Effat University, Jeddah 8482, Saudi Arabia

Corresponding author: Manal S. Esmail (manal.shaban.pg@eng.s-mu.edu.eg)

ABSTRACT Unmanned aerial vehicle quadcopters have applications in different real-life areas. They are nonlinear systems that necessitate the utilization of nonlinear control techniques. In this paper, we propose a new quaternion-based tracking controller for an underactuated quadcopter based on the pseudo linear feedback linearization technique. The quadcopter dynamic model was derived using Newton and Euler equations, and the global asymptotic stability of the quadcopter was verified using the Lyapunov stability criterion. The proposed controller has been compared to three state-of-the-art quadcopter controllers. Through simulation results, it has been shown that the proposed model has an effective and better performance than others. The metrics used in this evaluation are the steady-state error, maximum error, overshoot, and settling time. The different metrics proved the good performance of the proposed model in most of the different states that are presented.

INDEX TERMS Attitude and altitude tracking, feedback linearization, nonlinear control, quaternion tracking control, underactuated system.

I. INTRODUCTION

Quadcopters are among the most popular unmanned aerial vehicles as they can be utilized in various tasks, such as search and rescue operations [1], [2], military operations [3]–[5], and even agricultural processes (for spraying pesticides) [6], [7]. Moreover, the vertical take-off and landing capabilities, hover capability, great mobility, and agility of quadcopters make them extremely versatile in various operations. However, their usability still faces many control challenges, such as ensuring stable operation despite high nonlinearity, underactuated systems, strong coupling, external disturbance, and the need for fast control responses with satisfying regions of convergence in the presence of uncertainties [8], [9]. Controller development requires the development of a quadcopter dynamics mathematical model. A system dynamics model was previously obtained for a quadcopter using either the Newton–Euler or Euler–Lagrange methods [10], and the orientation of the quadcopter could be represented by rotation matrices, Euler angles, and quaternions. Quaternions were

employed in [11]–[14] to control the quadcopter attitude and position, and optimum performance was proven. Quaternions were also employed in some studies [15], [16] to solve the tracking problems of attitude and altitude with good performance. Moreover, the attitude tracking controller in [17]–[20] employed quaternions to avoid the issues of Euler angle representation.

In previous studies, variety of nonlinear techniques had been applied to quadcopters. For example, in [21], fuzzy PD and classical PD controllers were successfully implemented, and the performance of the Fuzzy PD controller was shown to be slightly better than the classical PD controller with regard to durability against noise and ease of implementation. To achieve good control for the position and the attitude of the quadcopter, a PID control technique has been proposed in [22]. The PID coefficients had been fine-tuned using a Genetic Algorithm (GA). The controller's robustness was evaluated in terms of sensor noise suppression, disturbance rejection, and sensitivity to model parameter uncertainty. The results of the robustness tests confirmed the efficacy and performance of the developed controller. A waypoint navigation controller was proposed in [23], using a fuzzy

The associate editor coordinating the review of this manuscript and approving it for publication was Zheng H. Zhu.

PID controller, which controlled a quadcopter to reach the desired position with good performance. In [24], a fuzzy PID controller was used instead of a traditional PID. Fuzzy controllers can improve quadcopter performance compared with classical PID controllers. In [25], the authors demonstrated how to adopt PID controllers in interference-enhanced models. Among the preferred techniques, solutions relying on a backstepping control technique using quaternion representation were proposed in [25]–[29]. The validity of the proposed controllers was verified by simulation and the Lyapunov stability criterion. In [31], a backstepping controller based on the Euler angle orientation technique was developed to control the altitude and attitude of quadcopter systems. The controller's validity was also assured by the Lyapunov function. The simulation results revealed transient and tracking responses with great precision. In [32], [33], LQR controllers were used to control the attitude and position of quadcopters using the Euler angle orientation approach. To increase the control algorithm responsiveness, the LQR controller was integrated with the feedback linearization model. The sliding mode has the benefit of solving uncertain issues in nonlinear system control. For example, in [34], an altitude controller was proposed based on the second-order sliding mode technique. It has good performance compared with three reference controllers. An adaptive sliding tracking controller in [35], achieved a low tracking error compared with a classical sliding mode controller. Attitude and altitude tracking controllers, which are based on a combination of sliding mode techniques and PID techniques were proposed in [36]. This controller was compared to other state-of-the-art (four types of sliding mode) [33], [34], [37], all of which use the same external disturbances. The proposed controller's efficacy is demonstrated by the simulation results. In [38], a combination of integral sliding mode and backstepping sliding mode controllers was established with uncertainties, and the presence of disturbances to track the attitude and position to achieve good tracking performance. In [39], a hybrid model by using integral backstepping and sliding mode controller is proposed for an efficient controller to track position and orientation by integrating a recursive control approach. Three state of the art [38]–[40] are implemented to compare with this controller to prove its efficiency.

Over the years, feedback linearization has attracted a lot of interest. In [42], the authors proposed a feedback linearization technique using a Luenberger observer to rebuild the no measured variables required to improve the robustness and performance of the proposed controller. The control system (i.e., observer, estimator, and controller) showed to have an interesting contribution for controlling the systems equipped with a minimum number of sensors. In [43], two sub controllers (i.e., feedback linearization and two PD controllers) were used to control the quadcopter. The proposed model could simultaneously combine tilting and movement along the desired trajectories, and the validity of the control system was tested by simulation. In [44], the authors proposed attitude, altitude, and position controller to keep the

quadcopter under control and stable. To prove the validity of this controller, it was compared with two state-of-the-art from the previous literature studies, and it was also tested experimentally. In [45], the authors presented a nonlinear output feedback control approach that achieved an asymptotic altitude and attitude trajectory tracking for a quadcopter system, and the external disruptions and model uncertainties were considered. To attain high performance and good stability, the authors in [46], proposed a hybrid model to control the position and the attitude of the quadcopter model. This model was linearized using feedback linearization approach, and a mixed sensitivity H∞ optimum controller was then built and synthesized. The controller was put to the test to see how well it can reject disturbances, reduce sensor noise, and deal with model uncertainties. In [47], the authors proposed a model based on feedback linearization side by side with backstepping. The proposed model presented satisfying results under high acceleration trajectory tracking and slowly varying wind conditions. Moreover, the authors in [48] proposed a hybrid system that relies on feedback linearization and LQR methods. The proposed technique was successful in tracking a predetermined trajectory and presenting small position errors under model inaccuracies, uncertainties, and disturbances. In our early work [49], the proposed controller task is to regulate the attitude and altitude of a quadcopter, but the regulation applications are less than the tracking applications. Also, new variables have been added to fit the proposed controller for tracking. The friction factor with air has also been added to make the proposed controller more realistic.

In this paper, the main contributions are as follows.

- A new quaternion-based feedback controller design is proposed for tracking quadcopter orientation and altitude.
- The proposed controller is not complex and allows low-end microcontroller-based implementations.
- A comparison with three controllers of the state-of-the-art quadcopter controllers (Non linear1, Non linear2, Non linear3) was conducted to demonstrate the effectiveness and performance of the proposed controller. The three controllers that were compared to the proposed model are summarized in the following three points.
  - ➢ Non linear1 controller achieved locally asymptotic stability [48]. Various aerodynamic and gyroscopic effects might be considered in quadcopter model. However, to keep the model as simple as possible, the authors ignored it. In altitude controller, it does not consider the first derivative of the desired altitude, this neglect has somewhat affected the performance compared to the proposed altitude controller.
  - ➢ Non linear2 controller achieved locally asymptotic stability [44]. It uses Euler angle representation that has singular configurations, in which the angular velocity loses one degree of freedom. These drawbacks can be avoided using unit quaternions that have proven good performance in comparison to the other representations.

➢ Non linear3 controller achieved almost global asymptotic stability [52]. It uses quaternion representation that achieved good performance compared to Non linear1, and Non linear2. This controller takes into consideration attitude tracking problem but doesn't consider the altitude tracking problem. Moreover, the gyroscopic moment, and various aerodynamic is not included in this controller.

- The gyroscopic moment, aerodynamic rotation, and translation drag are considered to achieve good accuracy. To the best of authors' knowledge, there are no solutions for attitude and altitude control in the literature used this technique without simplifying assumptions.
- The efficiency of the proposed controller is clearly shown when the quadcopter is in or near a corner pose due to use quaternion representation instead of Euler angle representation.
- The stability analysis of the proposed controller meets Lyapunov stability conditions.
- The proposed controller achieved global asymptotic stability.

The rest of this paper is organized as follows. The model, kinematics, and dynamics of the quadcopter are detailed in Section II. The flight controller design and stability analysis are presented in Section III. The simulation results of the proposed controller are presented and discussed in Section IV. Finally, the conclusion is mentioned in Section V.

II. SYSTEM DESIGN
A. QUADCOPTER STRUCTURE
In general, a quadcopter is a rigid body that is subjugated by its mass (m) and inertia (**J**). It is a flying vehicle with four propellers attached at the end of a cross frame, where one pair rotates clockwise, and the other pair rotates counterclockwise, both at equal distances from the vehicle center as shown in Fig.1. A body-fixed frame origin is typically placed to coincide with the center of mass. Around the normal direction, each propeller produces a normal force $\mathbf{F_i}$ and a moment $\mathbf{M_i}$. The mobility of the quadcopter is based on a fixed Earth frame with axes $[X\ Y\ Z]$. The origin vector of the quadcopter's body frame is set to $\mathbf{r} = [X_b\ Y_b\ Z_b]^T$. Moreover, $\dot{\mathbf{r}}$ denotes the quadcopter's velocity, $\ddot{\mathbf{r}}$ denotes its acceleration, and $\mathbf{\Omega}$ denotes its angular velocity. Moreover, $\mathbf{R}$ denotes the quadcopter rotation matrix with respect to the ground frame. The control of a quadcopter is performed by varying the speed of each rotor. To generate vertical take-off and landing, the four rotors' speeds are equal. To produce a rotation around the X-axis (roll rotation) coupled with motion along the Y-axis, the speed of the second and fourth rotors is changed. For a rotation around the Y-axis (pitch rotation) coupled with a motion along the X-axis, the speed of the first and third rotors is changed. To produce a rotation around the Z-axis (yaw rotation), the torque produced by each propeller pair must have a different polarity.
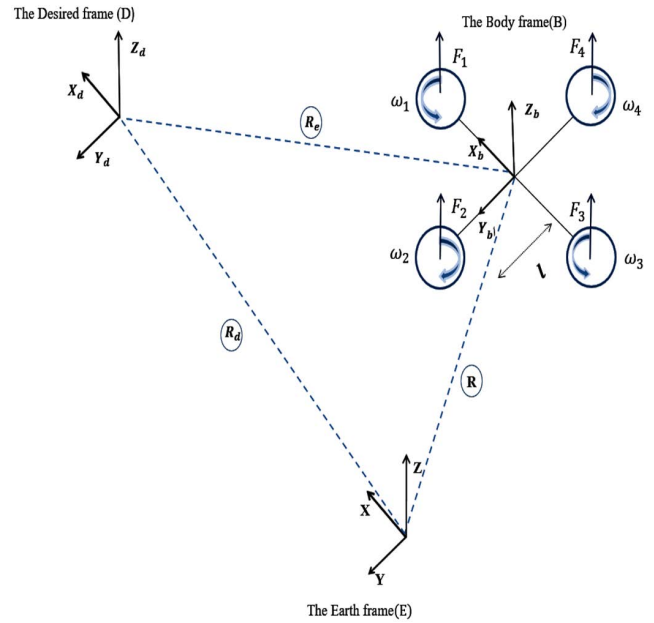

FIGURE 1. Quadcopter system coordinates.

B. KINEMATIC MODEL
Three coordinate frames are considered when building the mathematical model of a quadcopter: Earth fixed frame, body frame, and desired frame, as illustrated in Fig.1. The position and gravitational force of the quadcopter are measured in reference to the Earthfixed frame. However, the angular velocity and thrust of the quadcopter are measured in reference to the body frame. A unit quaternion $\mathbf{q}$ is used to represent the orientation of the body frame relative to the Earth frame [50]. For a body frame rotation about a unit axis $\mathbf{n}$ with an angle $-\pi < \theta < \pi$, a unit quaternion $\mathbf{q}$ is expressed as shown in (1).

$$q = \begin{bmatrix} \cos(\theta/2) \\ n\ \sin(\theta/2) \end{bmatrix} = \begin{bmatrix} q_0 \\ q_v \end{bmatrix} \tag{1}$$

The derivative of the quaternion is described by Eq. (2).

$$\dot{\mathbf{q}} = \mathbf{q} \otimes \mathbf{q}_\Omega \tag{2}$$

where $\mathbf{q}_\Omega = \begin{bmatrix} 0 \\ \Omega/2 \end{bmatrix}$ and the operator $\otimes$ is denoted for the quaternion multiplication operator and $\mathbf{\Omega}$ is the body frame angular velocity.

C. DYNAMICS
Two subsystems explain the dynamic model of the quadcopter body: a rotating subsystem (attitude) and a translational subsystem (altitude (z), x, and y). The Euler torque equation describes the rotational motion, while the Newton force describes the translational motion of the quadcopter body.

1) ROTATIONAL DYNAMICS
The rotational movement of the quadcopter is described in the body frame (i.e., to have the inertia matrix invariant with

time) by Eq. (3) as mentioned in [14].

$$J\dot{\Omega} + \Omega \times J\Omega + J_r\,\Omega \times \begin{bmatrix} 0 \\ 0 \\ \omega_r \end{bmatrix} + k_r\Omega = M_B \qquad (3)$$

where Ω denotes the vehicle's angular velocity, $J \in \mathbf{R}^{3\times3}$ is the symmetric positive definite moment of inertia matrix of the vehicle, J_r is the rotor' inertia, $\omega_r = \omega_1 - \omega_2 + \omega_3 - \omega_4$, k_r is the aerodynamic rotation drag coefficients, and M_B is the total torque acting on the quadrotor body.

2) TRANSLATIONAL DYNAMICS

The quadcopter's translation equations of motion are based on Newton's Second Law [51], and they are calculated with regard to the Earth's fixed frame[14], as shown in Eq. (4).

$$m\ddot{r} = mg \begin{bmatrix} 0 \\ 0 \\ 1 \end{bmatrix} + RF_b - k_t\dot{r} \qquad (4)$$

where k_t represents the aerodynamic translation drag coefficients.

$$F_b = \begin{bmatrix} 0 \\ 0 \\ F_b \end{bmatrix} = \begin{bmatrix} 0 \\ 0 \\ k_f\left(\omega_1^2 + \omega_2^2 + \omega_3^2 + \omega_4^2\right) \end{bmatrix} \qquad (5)$$

Assume that the propeller speeds can be instantly altered, and that the system has four inputs, M_B and F_b. The quadcopter system's input vector is specified as

$$U = [M_B F_b]^T = [u_1\ u_2\ u_3\ u_4]^T.$$

III. FEEDBACK LINEARIZATION CONTROL

In this section, the developed pseudo nonlinear feedback linearization tracking controller for the attitude and altitude of quadcopter systems is described. The quadcopter's nonlinear dynamics were converted into linear equivalent dynamics using the feedback linearization control technology. A block diagram of the feedback system is shown in Fig.2. In the beginning, a state-space model was derived. The actual angular velocity $\Omega = \begin{bmatrix} p & q & r \end{bmatrix}^T$, the orientation represented by the axis angle θ, position r, and velocity $\dot{r}$ were used as feedback signals. Moreover, the value of the desired angle θ_d, the desired angular velocity Ω_d, and the desired acceleration α_d were considered as inputs for the controller. The controller calculates the values of u_1, u_2, and u_3 to ensure that the quaternion error is equal to $q_e = [1\ 0\ 0\ 0]^T$. Additionally, it specifies the control input u_4 to ensure that the quadcopter altitude is equal to the desired altitude. Then, the propeller speeds ω_i are calculated depending on the values of u_1, u_2, u_3, and u_4.

A. ATTITUDE TRACKING CONTROL DESIGN

The attitude stability of quadcopters has drawn a lot of attention, and its value may be seen in both flexible and challenging movements. The attitude controller aims to ensure that the body frame is aligned with the desired frame. For this
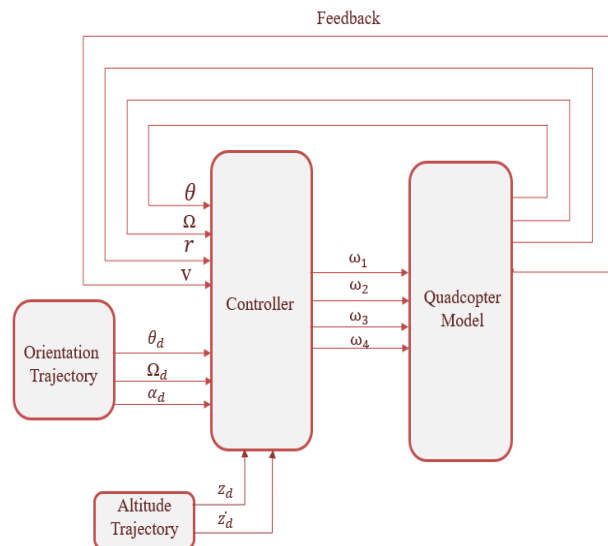

FIGURE 2. Structure of the overall control system.

reason, the desired attitude of a quadcopter is represented by the desired frame, which is denoted by $[X_d\ Y_d\ Z_d]$. The corresponding rotation matrix ofthe desired frame with respect to the Earth frame is denoted by $R_d \in$ SO (3).The desired unit quaternion is defined as $q_d = \begin{bmatrix} q_{0d}, & q_{vd} \end{bmatrix}$, which is used to describe the orientation of the desired frame with respect to the Earth fame. The relationship between the coordinate frames is shown in Fig. 1. The desired angular velocity, which is denoted by Ω_d, is the angular velocity of the desired body frame. A quaternion error must be defined to design an attitude tracking controller. The quaternion error q_e is to measure the discrepancy between the desiredquaternion q_d and the actual quaternion q. q_e is defined by Eq. (6).

$$q_e = q_d{}^* \otimes q \qquad (6)$$

To reach the desired orientation, rotation by the quaternion error q_e is required. To calculate the time derivative of q_e, both sides of the above equation are differentiated with respect to time.

$$\dot{q}_e = \frac{d}{dt}(q_d{}^* \otimes q) = (\dot{q}_d{}^*) \otimes q + q_d{}^* \otimes \dot{q} \qquad (7)$$

The time derivative of q_d is defined as in Eq. (2) and is given by the following form:

$$\dot{q}_d = q_d \otimes q_{\Omega d} \qquad (8)$$

Taking the conjugate of the time derivative of the q_d equation leads to:

$$(\dot{q}_d)^* = (q_d \otimes q_{\Omega d})^* = q_{\Omega d}{}^* \otimes q_d{}^* \qquad (9)$$

Eq. (7) in view of Eq. (2) and Eq. (8) leads to:

$$\dot{q}_e = q_{\Omega d}{}^* \otimes q_d{}^* \otimes q + q_d{}^* \otimes q \otimes q_\Omega \qquad (10)$$

The time derivative of the unit quaternion error is also defined like that of $\dot{q}$.

$$\dot{\mathbf{q}}_{\mathbf{e}} = \mathbf{q}_{\mathbf{e}} \otimes \mathbf{q}_{\Omega\mathbf{e}} \tag{11}$$

By substituting Eq. (11) into Eq. (10),

$$\mathbf{q}_{\Omega\mathbf{d}}{}^* \otimes \mathbf{q}_{\mathbf{d}}{}^* \otimes \mathbf{q} + \mathbf{q}_{\mathbf{d}}{}^* \otimes \mathbf{q} \otimes \mathbf{q}_{\Omega} = \mathbf{q}_{\mathbf{e}} \otimes \mathbf{q}_{\Omega\mathbf{e}}$$

Multiplying by $q_e{}^*$ leads to:

$$\mathbf{q}_{\mathbf{e}}{}^* \otimes \mathbf{q}_{\Omega\mathbf{d}}{}^* \otimes \mathbf{q}_{\mathbf{d}}{}^* \otimes \mathbf{q} + \mathbf{q}_{\mathbf{e}}{}^* \otimes \mathbf{q}_{\mathbf{d}}{}^* \otimes \mathbf{q} \otimes \mathbf{q}_{\Omega} = \mathbf{q}_{\Omega\mathbf{e}} \tag{12}$$

On substituting the value of $\mathbf{q}_{\mathbf{e}}^*$,

$$\mathbf{q}^* \otimes \mathbf{q}_{\mathbf{d}} \otimes \mathbf{q}_{\Omega\mathbf{d}}{}^* \otimes \mathbf{q}_{\mathbf{d}}{}^* \otimes \mathbf{q} + \mathbf{q}^* \otimes \mathbf{q}_{\mathbf{d}} \otimes \mathbf{q}_{\mathbf{d}}{}^* \otimes \mathbf{q} \otimes \mathbf{q}_{\Omega} = \mathbf{q}_{\Omega\mathbf{e}} \tag{13}$$

The above equation is simplified using the properties of quaternion multiplications, i.e., $\mathbf{q}^* \otimes \mathbf{q}_{\mathbf{d}} \otimes \mathbf{q}_{\mathbf{d}}{}^* \otimes \mathbf{q} = 1$ gives:

$$-\mathbf{q}^* \otimes \mathbf{q}_{\mathbf{d}} \otimes \mathbf{q}_{\Omega\mathbf{d}} \otimes \mathbf{q}_{\mathbf{d}}{}^* \otimes \mathbf{q} + \mathbf{q}_{\Omega} = \mathbf{q}_{\Omega\mathbf{e}} \tag{14}$$

The term: $\mathbf{q}^* \otimes \mathbf{q}_{\mathbf{d}} \otimes \mathbf{q}_{\Omega\mathbf{d}} \otimes \mathbf{q}_{\mathbf{d}}{}^* \otimes \mathbf{q} = (\mathbf{q}^* \otimes \mathbf{q}_{\mathbf{d}}) \otimes \mathbf{q}_{\Omega\mathbf{d}} \otimes$ $(\mathbf{q}^* \otimes \mathbf{q}_{\mathbf{d}})^*$ with $\mathbf{q}_{\Omega\mathbf{d}} = \begin{bmatrix} 0 \\ \Omega_{\mathbf{d}}/2 \end{bmatrix}$ can be interpreted as the rotation of the vector $\Omega_{\mathbf{d}}/2$ by the rotation described by $\mathbf{q}^* \otimes \mathbf{q}_{\mathbf{d}}$. Hence, we have:

$$(\mathbf{q}^* \otimes \mathbf{q}_{\mathbf{d}}) \otimes \mathbf{q}_{\Omega\mathbf{d}} \otimes (\mathbf{q}^* \otimes \mathbf{q}_{\mathbf{d}})^* = \begin{bmatrix} 0 \\ \mathbf{R}^{\mathbf{T}}\mathbf{R}_{\mathbf{d}}\Omega_{\mathbf{d}}/2 \end{bmatrix}$$

The mismatch between the rotation $\mathbf{R}$ and $\mathbf{R}_{\mathbf{d}}$ matrices is defined by $\mathbf{R}_{\mathbf{e}} = \mathbf{R}_{\mathbf{d}}^{\mathbf{T}}\mathbf{R}$.

The following equation is the dynamical equation for the angular velocity tracking error $\Omega_{\mathbf{e}} \in \mathbf{R}^3$

$$\Omega_{\mathbf{e}} = \Omega - \mathbf{R}^{\mathbf{T}}\mathbf{R}_{\mathbf{d}}\Omega_{\mathbf{d}} = \Omega - \mathbf{R}_{\mathbf{e}}^{\mathbf{T}}\Omega_{\mathbf{d}} \tag{15}$$

The quadcopter system's variables were changed from $\Omega_{\mathbf{e}}$ and $\mathbf{q}_{\mathbf{e}}$ to $\Omega_{\mathbf{e}}$ and $\mathbf{x}_{\mathbf{e}}$, where $\mathbf{x}_{\mathbf{e}}$ is defined as follows.

$$\mathbf{x}_{\mathbf{e}} = \Omega_{\mathbf{e}} + k_1\mathbf{q}_{\mathbf{ve}} = \Omega_{\mathbf{e}} + k_1\mathbf{M}\mathbf{q}_{\mathbf{e}} \tag{16}$$

where $\mathbf{M} = \begin{bmatrix} 0 & 1 & 0 & 0 \\ 0 & 0 & 1 & 0 \\ 0 & 0 & 0 & 1 \end{bmatrix}$, and k_1 is a positive constant. The state equation of x_e is given by Eq. (17):

$$\mathbf{J}\dot{\mathbf{x}}_{\mathbf{e}} = \mathbf{J}\dot{\Omega}_{\mathbf{e}} + k_1\mathbf{J}\mathbf{M}\dot{\mathbf{q}}_{\mathbf{e}} \tag{17}$$

To calculate $\dot{\Omega}_{\mathbf{e}}$, both sides of Eq. (15) are differentiated with respect to time as follows:

$$\dot{\Omega}_{\mathbf{e}} = \dot{\Omega} - (\mathbf{R}_{\mathbf{e}}^{\mathbf{T}}\Omega_{\dot{\mathbf{d}}}) = \dot{\Omega} - (\dot{\mathbf{R}}_{\mathbf{e}}^{\mathbf{T}}\Omega_{\mathbf{d}} + \mathbf{R}_{\mathbf{e}}^{\mathbf{T}}\dot{\Omega}_{\mathbf{d}})$$

The state equation of $\Omega_{\mathbf{e}}$ is represented in the body frame as follows:

$$\dot{\Omega}_{\mathbf{e}} = \dot{\Omega} + \Omega \times \mathbf{R}_{\mathbf{e}}^{\mathbf{T}}\Omega - \mathbf{R}_{\mathbf{e}}^{\mathbf{T}}\dot{\Omega}_{\mathbf{d}} \tag{18}$$

By substituting Eq. (18) into Eq. (3), the following equation is obtained:

$$\mathbf{J}\dot{\Omega}_{\mathbf{e}} + \mathbf{J}\left(-\Omega \times \mathbf{R}_{\mathbf{e}}^{\mathbf{T}}\Omega + \mathbf{R}_{\mathbf{e}}^{\mathbf{T}}\Omega_{\mathbf{d}}.\right) + \Omega \times \mathbf{J}\Omega + \mathbf{J}_{\mathbf{r}}\Omega$$
$$\times \begin{bmatrix} 0 \\ 0 \\ \omega_{\mathbf{r}} \end{bmatrix} = \mathbf{M}_{\mathbf{B}} \tag{19}$$

Eq. (19) in view of Eq. (17) leads to the following equation:

$$\mathbf{J}\dot{\mathbf{x}}_{\mathbf{e}} = k_1\mathbf{J}\mathbf{M}\mathbf{q}_{\mathbf{e}} \otimes \mathbf{q}_{\Omega_{\mathbf{e}}} - \mathbf{J}(-\Omega \times \mathbf{R}_{\mathbf{e}}^{\mathbf{T}}\Omega + \mathbf{R}_{\mathbf{e}}^{\mathbf{T}}\dot{\Omega}_{\mathbf{d}})$$
$$- \Omega \times \mathbf{J}\Omega - \mathbf{J}_{\mathbf{r}}\,\Omega \times \begin{bmatrix} 0 \\ 0 \\ \omega_{\mathbf{r}} \end{bmatrix} + \mathbf{M}_{\mathbf{B}} \tag{20}$$

In the state space of $\Omega_{\mathbf{e}}$ and $\mathbf{x}_{\mathbf{e}}$, Eq. (19) with Eq. (20) define the quadcopter rotational dynamics. The control law of the quadcopter orientation is denoted by Eq. (21):

$$\mathbf{M}_{\mathbf{B}} = -k_1\mathbf{J}\mathbf{M}\mathbf{q}_{\mathbf{e}} \otimes \mathbf{q}_{\Omega_{\mathbf{e}}} - k_2\mathbf{x}_{\mathbf{e}} + \mathbf{J}(-\Omega \times \mathbf{R}_{\mathbf{e}}^{T}\Omega + \mathbf{R}_{\mathbf{e}}^{T}\dot{\Omega}_{\mathbf{d}})$$
$$+ \Omega \times \mathbf{J}\Omega + \mathbf{J}_{\mathbf{r}}\,\Omega \times \begin{bmatrix} 0 \\ 0 \\ \omega_{\mathbf{r}} \end{bmatrix} \tag{21}$$

By substituting Eq. (21) into Eq. (19) and Eq. (20), Eqs. (22) and (23) are obtained.

$$\mathbf{J}\dot{\mathbf{x}}_{\mathbf{e}} = -k_2\mathbf{x}_{\mathbf{e}} \tag{22}$$
$$\mathbf{J}\dot{\Omega}_{\mathbf{e}} = -k_2\mathbf{x}_{\mathbf{e}} - k_1\mathbf{J}\mathbf{M}\mathbf{q}_{\mathbf{e}} \otimes \mathbf{q}_{\Omega_{\mathbf{e}}} \tag{23}$$

Eqs. (22) and (23) describe the system model that has equilibrium points at $\mathbf{x}_{\mathbf{e}} = 0$ and $\Omega_{\mathbf{e}} = 0$, which is equivalent to $\mathbf{q}_{\mathbf{e}} = [\pm 1\ 0\ 0\ 0]^{\mathrm{T}}$ and $\Omega_{\mathbf{e}} = 0$ to be stable.

B. STABILITY ANALYSIS

The Lyapunov stability theorem was utilized to demonstrate the correctness of this controller. The candidate Lyapunov function $V(\mathbf{x}_{\mathbf{e}}, \Omega_{\mathbf{e}})$ is defined as follows.

$$V(\mathbf{x}_{\mathbf{e}}, \Omega_{\mathbf{e}}) = 0.5(\mathbf{M}\mathbf{q}_{\mathbf{e}})^{\mathrm{T}}\mathbf{M}\mathbf{q}_{\mathbf{e}} + 0.5\mathbf{x}_{\mathbf{e}}^{\mathrm{T}}\mathbf{J}\mathbf{x}_{\mathbf{e}} \tag{24}$$

Substituting for Mq_e from Eq. (16) gives

$$V(\mathbf{x}_{\mathbf{e}}, \Omega_{\mathbf{e}}) = \frac{1}{k_1^2}0.5(\mathbf{x}_{\mathbf{e}} - \Omega_{\mathbf{e}})^{\mathrm{T}}(\mathbf{x}_{\mathbf{e}} - \Omega_{\mathbf{e}}) + 0.5\mathbf{x}_{\mathbf{e}}^{\mathrm{T}}\mathbf{J}\mathbf{x}_{\mathbf{e}}$$

The Lyapunov function $V(\mathbf{x}_{\mathbf{e}}, \Omega_{\mathbf{e}})$ is positive definite because the $\mathbf{J}$ matrix is positive definite. Also, $V(\mathbf{x}_{\mathbf{e}}, \Omega_{\mathbf{e}}) = 0$ if and only if $\mathbf{x}_{\mathbf{e}} = 0$ and $\Omega_{\mathbf{e}} = 0$. Thus, the first two conditions for the Lyapunov function validity are verified. To verify the stability of the proposed controller, we must prove that the time derivative of $V(\mathbf{x}_{\mathbf{e}}, \Omega_{\mathbf{e}})$ is negative in a domain that encloses the equilibrium point.

The time derivative of $V(\mathbf{x}_{\mathbf{e}}, \Omega_{\mathbf{e}})$ is given by

$$\dot{V}(\mathbf{x}_{\mathbf{e}}, \Omega_{\mathbf{e}}) = \frac{1}{k_1^2}(\mathbf{x}_{\mathbf{e}} - \Omega_{\mathbf{e}})^{\mathrm{T}}(\dot{\mathbf{x}}_{\mathbf{e}} - \dot{\Omega}_{\mathbf{e}}) + \mathbf{x}_{\mathbf{e}}^{\mathrm{T}}\mathbf{J}\dot{\mathbf{x}}_{\mathbf{e}} \tag{25}$$

whose time derivative in view of Eq. (22) and Eq. (23) is given by

$$\dot{V}(\mathbf{x}_{\mathbf{e}}, \Omega_{\mathbf{e}}) = \frac{1}{k_1^2}(\mathbf{x}_{\mathbf{e}} - \Omega_{\mathbf{e}})^{\mathrm{T}}(k_1\mathbf{M}\dot{\mathbf{q}}_{\mathbf{e}}) - k_2\mathbf{x}_{\mathbf{e}}^{\mathrm{T}}\mathbf{x}_{\mathbf{e}} \tag{26a}$$

In view of Eq. (16), and Eq.(11), Eq. (26a) can be simplified to:

$$\dot{V}\left(\mathbf{x_e}, \boldsymbol{\Omega_e}\right) = \left(\mathbf{Mq_e}\right)^T \left(\mathbf{Mq_e} \otimes \mathbf{q_{\Omega e}}\right) - k_2 \mathbf{x_e^T x_e} \quad (26b)$$

where $\mathbf{q_e} = \left[q_{0e}, \mathbf{q_{ve}}\right]^T$, and $\mathbf{Mq_e} = \mathbf{q_{ve}}$.

By substituting for $\mathbf{q_e}$ and $\mathbf{q_{\Omega e}}$ in the previous equation, then

$$\dot{V}\left(\mathbf{x_e}, \boldsymbol{\Omega_e}\right) = \mathbf{q_{ve}^T M} \left(\begin{bmatrix} q_{0e} \\ \mathbf{q_{ve}} \end{bmatrix} \otimes \begin{bmatrix} 0 \\ \boldsymbol{\Omega_e}/2 \end{bmatrix} \right) - k_2 \mathbf{x_e^T x_e} \quad (26c)$$

After some quaternion multiplications, one can deduce that:

$$\dot{V}\left(\mathbf{x_e}, \boldsymbol{\Omega_e}\right) = \frac{1}{2} \mathbf{q_{ve}^T M} \left(\begin{bmatrix} -\mathbf{q_{ve}^T \Omega_e} \\ q_{0e}\boldsymbol{\Omega_e} + \mathbf{q_{ve}} \times \boldsymbol{\Omega_e} \end{bmatrix} \right) - k_2 \mathbf{x_e^T x_e} \quad (26d)$$

After the simplification of the first term in the RHS, $\dot{V}\left(\mathbf{x_e}, \boldsymbol{\Omega_e}\right)$ can be written as follows:

$$\dot{V}\left(\mathbf{x_e}, \boldsymbol{\Omega_e}\right) = \frac{1}{2} \mathbf{q_{ve}^T} \left(q_{0e}\boldsymbol{\Omega_e} + \mathbf{q_{ve}} \times \boldsymbol{\Omega_e}\right) - k_2 \mathbf{x_e^T x_e} \quad (26e)$$

Further simplification leads to:

$$\dot{V}\left(\mathbf{x_e}, \boldsymbol{\Omega_e}\right) = \frac{q_{0e}}{2} \mathbf{q_{ve}^T \Omega_e} - k_2 \mathbf{x_e^T x_e} \quad (26f)$$

Let $\boldsymbol{\Omega_e} = \boldsymbol{\Omega_{pe}} + \boldsymbol{\Omega_{ne}}$, where $\boldsymbol{\Omega_{pe}}$ is the parallel component to the vector $\mathbf{q_{ve}}$, and $\boldsymbol{\Omega_{ne}}$ is the normal component to the vector $\mathbf{q_{ve}}$. The control parameters k_1 and k_2 are always positive. Therefore, $\boldsymbol{\Omega_{pe}}$ and $\boldsymbol{\Omega_{ne}}$ can be defined as follows:

$$\boldsymbol{\Omega_{pe}} = \alpha_1 k_1 \mathbf{q_{ve}}$$
$$\boldsymbol{\Omega_{ne}} = \boldsymbol{\Omega} - \boldsymbol{\Omega_{pe}}$$

where α_1 is a real constant. By substituting $\boldsymbol{\Omega_{pe}}$ and $\boldsymbol{\Omega_{ne}}$ in Eq.(26f),

$$\dot{V}\left(\mathbf{x_e}, \boldsymbol{\Omega_e}\right) = 0.5\alpha_1 k_1 q_{0e} \mathbf{q_{ve}^T q_{ve}} - k_2 \mathbf{x_e^T x_e}$$

Substituting for $\mathbf{x_e}$ gives:

$$\dot{V}\left(\mathbf{x_e}, \boldsymbol{\Omega_e}\right) = 0.5\alpha_1 k_1 q_{0e} \mathbf{q_{ve}^T q_{ve}} - k_2 \left(\boldsymbol{\Omega_e} + k_1 \mathbf{q_{ve}}\right)^T$$
$$\times \left(\boldsymbol{\Omega_e} + k_1 \mathbf{q_{ve}}\right) \quad (26g)$$

The $\mathbf{x_e^T x_e}$ term can be defined by the parallel and normal components of $\boldsymbol{\Omega_e}$ as follows:

$$\left(\boldsymbol{\Omega_e} + k_1 \mathbf{q_{ve}}\right)^T \left(\boldsymbol{\Omega_e} + k_1 \mathbf{q_{ve}}\right)$$
$$= \left(\boldsymbol{\Omega_{ne}} + \boldsymbol{\Omega_{pe}} + k_1 \mathbf{q_{ve}}\right)^T \left(\boldsymbol{\Omega_{ne}} + \boldsymbol{\Omega_{pe}} + k_1 \mathbf{q_{ve}}\right) \quad (27)$$

where $\mathbf{q_{ve}}$ and $\boldsymbol{\Omega_{ne}}$ are normal. Therefore,

$$\left(\boldsymbol{\Omega_e} + k_1 \mathbf{q_{ve}}\right)^T \left(\boldsymbol{\Omega_e} + k_1 \mathbf{q_{ve}}\right)$$
$$= \boldsymbol{\Omega_{ne}^T \Omega_{ne}} + \left(\alpha_1 + 1\right)^2 k_1^2 \mathbf{q_{ve}^T q_{ve}} \quad (28)$$

By substituting Eq. (28) into Eq. (26g), $\dot{V}\left(\mathbf{x_e}, \boldsymbol{\Omega_e}\right)$ becomes

$$\dot{V}\left(\mathbf{x_e}, \boldsymbol{\Omega_e}\right) = 0.5\alpha_1 k_1 q_{0e} \mathbf{q_{ve}^T q_{ve}} - k_2 \boldsymbol{\Omega_{ne}^T \Omega_{ne}}$$
$$- k_2 \left(\alpha_1 + 1\right)^2 k_1^2 \mathbf{q_{ve}^T q_{ve}}$$

This may be expressed in the following manner:

$$\dot{V}\left(\mathbf{x_e}, \boldsymbol{\Omega_e}\right) = -k_1 \left(k_1 k_2 \left(\alpha_1 + 1\right)^2 - 0.5\alpha_1 q_{0e}\right) \mathbf{q_{ve}^T q_{ve}}$$
$$- k_2 \boldsymbol{\Omega_{ne}^T \Omega_{ne}}$$

where $\dot{V}\left(\mathbf{x_e}, \boldsymbol{\Omega_e}\right)$ should be positive definite to meet the Lyapunov stability requirement and the controller parameters k_1, k_2 are assumed to always be positive. Hence, $\dot{V}\left(\mathbf{x_e}, \boldsymbol{\Omega_e}\right)$ is positive definite if $k_1 k_2 \left(\alpha_1 + 1\right)^2 - 0.5\alpha_1 q_{0e} > 0$, which can be simplified as follows:

$$\alpha_1^2 + \left(2 - \frac{q_{0e}}{2k_1 k_2}\right)\alpha_1 + 1 > 0 \quad (29)$$

This equation's discriminator is given by:

$$D = \left(1 - \frac{q_{0e}}{4k_1 k_2}\right)^2 - 1 \quad (30)$$

where q_{0e} is constrained to be positive. Hence, if $0 < \frac{q_{0e}}{4k_1 k_2} < 2$, D is smaller than zero (D < 0), implying that the requirement given in Eq. (29) can be held for any value of α_1. Given that $q_{0e} < 1$, by putting the constraint $k_1 k_2 > \frac{1}{8}$ on the system, for any values of $\mathbf{q_e}$ and $\boldsymbol{\Omega_e}$, the system can be stabilized. Finally, $\dot{V}\left(\mathbf{x_e}, \boldsymbol{\Omega_e}\right)$ is deduced as follows:

$$\dot{V}\left(\mathbf{x_e}, \boldsymbol{\Omega_e}\right) = -k_{12} \mathbf{q_{ve}^T q_{ve}} - k_2 \boldsymbol{\Omega_{ne}^T \Omega_{ne}} \quad (31)$$

where the constant $k_{12} = k_1 \left(k_1 k_2 \left(\alpha_1 + 1\right)^2 - 0.5\alpha_1 q_{0e}\right)$ is positive if the constants k_1 and k_2 satisfy the condition that $k_1 k_2 > \frac{1}{8}$. Hence, $\dot{V}\left(\mathbf{x_e}, \boldsymbol{\Omega_e}\right) \leq 0$. Also, it may be demonstrated that $\dot{V}\left(\mathbf{x_e}, \boldsymbol{\Omega_e}\right) = 0$ only if $\mathbf{x_e} = 0$ and $\boldsymbol{\Omega_e} = 0$. Global asymptotic stability is achieved if these requirements are met.

C. ALTITUDE CONTROLLER

In this section, we describe the designed feedback control scheme for the altitude stabilization of the quadcopter. To this end, Eq. (6) was used; however, we were concerned with controlling the altitude z. As a result, the used quadcopter altitude dynamics equation is expressed as follows:

$$m\ddot{z} = -mg + r_{33}F_b - k_t \dot{z} \quad (32)$$

where r_{33} is the last row and last column element of the rotation matrix $\mathbf{R}$.

Eq. (32) can be linearized by applying the following control law:

$$F_b = \frac{mg + v + k_t \dot{z}}{r_{33}}$$

where v is a newly added control input. This change is correct whenever $r_{33} \neq 0$. In a modified form, the altitude dynamics may be stated as follows

$$m\ddot{z} = v \quad (33)$$

Eq. (33) represents an ordinary linear system with a control input v. It may be utilized to stabilize a system like this by employing a PD controller in the following way:

$$v = -k_3(z - z_d) - k_4(\dot{z} - \dot{z}_d) \quad (34)$$

where z_d is the desired altitude.

TABLE 1. Quadcopter parameters and constant.

Parameter	Description	Value
J_x	MOI about x-axis	$7.5e\text{-}3\ kg.m^2$
J_y	MOI about y-axis	$7.5e\text{-}3\ kg.m^2$
J_z	MOI about z-axis	$1.3e\text{-}3\ kg.m^2$
J_r	Inertia of motor	$6e\text{-}5\ kg.m^2$
l	Moment arm	$0.23\ m$
m	Quadcopter mass	$0.65\ kg$
k_f	Thrust coefficient	$3.13e\text{-}5\ N\,s^2$
k_M	Moment coefficient	$7.5e\text{-}7\ N\,ms^2$
k_r	Rotation drag coefficient	$diag\ (0.1, 0.1, 0.15)\ Nm.s$
k_t	Translation drag coefficient	$diag\ (0.1, 0.1, 0.15)\ Ns/m$
g	gravitational acceleration	$9.81\ m/s^2$

A good combination of k_3 and k_4 can stabilize the system indicated by Eq. (34). The following equation describes the altitude control law:

$$F_b = \frac{mg - k_3(z - z_d) - k_4(\dot{z} - \dot{z}_d) - k_t\dot{z}}{r_{33}}$$

The attitude controller is independent from the altitude controller, but the attitude affects the altitude controller. As the quadcopter orientation gets nearly vertical, we lose the ability to control the altitude because propellers forces are nearly horizontal. If the quadcopter orientations change by more than 90 degs, the propellers effectively push the quadcopter down in the same direction of gravity force; therefore, we cannot control the quadcopter altitude.

IV. SIMULATION RESULTS

This study is a follow-up to a previous publication [49] whose task is to regulate the attitude and altitude of a quadcopter. In this part, we compare the proposed tracking controller to the three state-of-the-art controllers (Non linear1, Non linear2, Non linear3) described in [48], [44], and [52], respectively. A case study is conducted on a quadcopter with physical parameters provided in [53].Hence the initial conditions and nominal parameters have been presented in Table 1. The simulations were run on a PC with 8GB of RAM, a 64-bit operating system, and an Intel(R)z Core (TM) i5-10300H CPU running at 2.50GHz.

For the proposed controller, the value of the control parameters is determined to improve the step responses by selecting a suitable value for the settling time and overshoot

(2 sec, 5%), then the system poles are determined to achieve this performance. The gains are determined based on the value of the obtained poles. Then, the authors performed fine tuning and selected the proper value of the gain to get the best performance under the conditions that we deduced from the Lyapunov theory, which states that ($k_1 k_2 > \frac{1}{8}$). We applied the control law of the proposed controller (attitude and altitude) with a constant ($k_1 \sim k_4 = 4$).

A. THREE STATE OF THE ART CONTROLLERS
1) NON LINEAR1 CONTROLLER EQUATION
The first controller's equation (Non linear1) is expressed as follows [48]:

$$\mathbf{u_{in}} = -\mathbf{\Lambda}^{-1}(\mathbf{x_{in}})\,\mathbf{b_{in}}(\mathbf{x_{in}}) + \mathbf{\Lambda}^{-1}(\mathbf{x_{in}})\,V_{in}$$

where $\mathbf{u_{in}}$ denotes the system's vector of inputs $\mathbf{u_{in}} = \begin{bmatrix} F_b & \mathbf{M_B} \end{bmatrix}$, and $\mathbf{\Lambda}(\mathbf{x_{in}})$ is the decoupling matrix, which is defined as follows:

$$\mathbf{\Lambda}(\mathbf{x_{in}}) = \begin{bmatrix} \dfrac{c_\theta c_\phi}{m} & 0 & 0 & 0 \\ 0 & \dfrac{1}{J_x} & \dfrac{t_\theta s_\phi}{J_y} & \dfrac{c_\phi t_\theta}{J_z} \\ 0 & 0 & \dfrac{c_\phi}{J_y} & -\dfrac{s_\phi}{J_z} \\ 0 & 0 & \dfrac{s_\phi}{J_y c_\theta} & \dfrac{c_\phi}{J_z c_\theta} \end{bmatrix}$$

$$\mathbf{b_{in}}(\mathbf{x_{in}}) = \begin{bmatrix} -g & \dot{\theta}\dot{\psi}\left(\dfrac{J_y - J_z}{J_x}\right) & \dot{\phi}\dot{\psi}\left(\dfrac{J_z - J_x}{J_y}\right) & \dot{\phi}\dot{\theta}\left(\dfrac{J_y - J_z}{J_x}\right) \end{bmatrix}^T$$

where c, s, and t are shorthand forms for the cosine, sine, and tangent functions, respectively. $\mathbf{x_{in}}$ is the vector of state variables $\mathbf{x_{in}} = \begin{bmatrix} z & \phi & \theta & \psi & \dot{z} & p & q & r \end{bmatrix}^T$ .V_{in} is the transformed input variables vector obtained from four single-input single-output chains of two integrators.

For Non linear1, analyzing the step responses was used to evaluate the gains. The Q and R matrices used in each subsystem's optimum gains computation are listed in Table 2 in [48].

2) NON LINEAR2 CONTROLLER EQUATION
The second controller's equation (Non linear2) is expressed as follows [44], $\mathbf{M_B}$ and F_b, as shown at the bottom of the next page, where (ϕ, θ, ψ) denotes the rotations around the X, Y, and Z axes to characterize the quadcopter's orientation, and $c_1 \sim c_8$ are positive constants.The terms $e_1 \sim e_8$ refer to the errors related to the attitude and altitude dynamics, which could be determined using the below formulas.

$$e_1 = \phi - \phi_d$$
$$e_2 = \dot{\phi} - \dot{\phi}_d + c_1 e_1$$
$$e_3 = \theta - \theta_d$$
$$e_4 = \dot{\theta} - \dot{\theta}_d + c_3 e_3$$
$$e_5 = \psi - \psi_d$$
$$e_6 = \dot{\psi} - \dot{\psi}_d + c_5 e_5$$
$$e_7 = z - z_d$$
$$e_8 = \dot{z} - \dot{z}_d + c_7 e_7$$

TABLE 2. The settling time for the proposed system and the controllers in [48], [44], and [52] for step trajectory.

case	Controller	Settling time(s)			
		θ_x	θ_y	θ_z	Z
1	Proposed	1.77	Na	Na	**0**
	Nonlinear1	**0.63**	Na	Na	12.42
	Nonlinear2	3.63	Na	Na	19.54
	Nonlinear3	0.69	Na	Na	Na
2	Proposed	Na	Na	0.909	**0**
	Nonlinear1	Na	Na	1.83	5.98
	Nonlinear2	Na	Na	11.6	3.63
	Nonlinear3	Na	Na	**0.747**	Na
3	Proposed	Na	Na	Na	**4.15**
	Nonlinear1	Na	Na	Na	7.67
	Nonlinear2	Na	Na	Na	5.38
	Nonlinear3	Na	Na	Na	Na
4	Proposed	1.70	0	1.85	**3.77**
	Nonlinear1	1.6	0	1.53	8.26
	Nonlinear2	6.88	8.43	8.33	15.7
	Nonlinear3	**0.954**	0.46	**0.56**	Na

For Non linear2, the following values had been chosen for the control parameters: $c_1 \sim c_4 = 2.5$, c_5 $c_6 = 2$, $c_7 = 2.2$, $c_8 = 0.5$ (see simulation results section in [44]).

3) NON LINEAR3 CONTROLLER EQUATION
The third controller's equation (Non linear3) is expressed as follows [52].

$$\mathbf{M_B} = -\alpha_1 \mathbf{q^e} - \alpha_2 \mathbf{q}^\sim + \mathbf{JR^T}\left(\mathbf{Q^e}\right)\dot{\Omega}_\mathbf{d} + \mathbf{S(\Omega_d^-)J\Omega_d^-}$$

The constants α_1 and α_2 are both positive constants. The vector parts of the unit quaternions Q^e and $Q^\sim$ *are* q^e and $q^\sim$, respectively. The unit quaternion tracking error Q^e is the difference between the actual unit quaternion $\mathbf{Q}$ and the desired unit quaternion Q^d. The difference between the unit quaternion tracking error Q^e and the auxiliary feedback unit quaternion signal Q^- is denoted by the letter $Q^\sim$. For this controller, Q^- is the output of the auxiliary system.

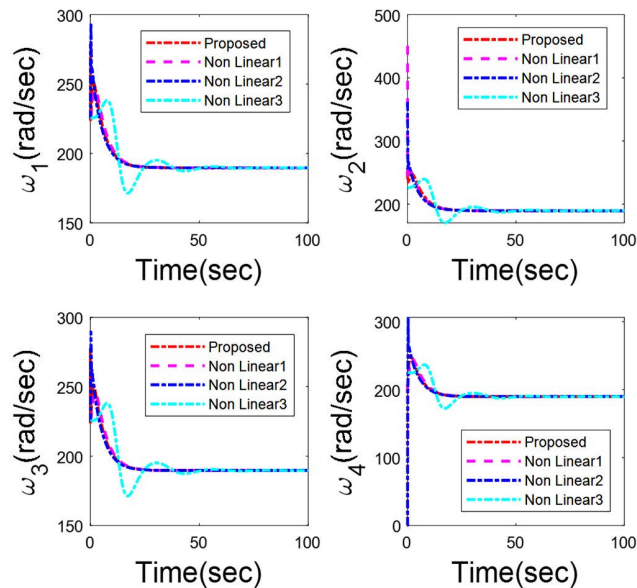**FIGURE 3.** Rotors speedaction for response to desired $\theta_{dx} = 45°$ for the proposed system and the controllers proposed in [48], [44], and [52].

For Non linear3, the following values had been chosen for the control parameters: α_1 and $\alpha_2 = 30$ (see simulation results section in [52]).

B. ACTUATOR EFFORTS
The propeller speeds (which represent actuator efforts) for the proposed controller and the other three candidate controllers are shown in Fig. 3 for a step-change in orientation by $\theta_{dx} = 45°$. The propeller speeds must at least support the quadcopter weight and extra loading due to quadcopter dynamics and air friction. Practical propeller actuators have a physical speed limit. This speed limit is included in our simulation model (450 rad/s).

C. RESPONSE TO VARIOUS TRAJECTORY
The performances of the four controllers are evaluated through some trajectories, such as step trajectory inFig.4, ramp trajectory in Fig.5, and parabolic trajectory in Fig.6. The performances of all controllers along step trajectory, ramp trajectory, and parabolic trajectory are illustrated in chronological order. Four cases are studied to prove the sta-

$$\mathbf{M_B} = \begin{bmatrix} \frac{J_x}{l}(-\dot{\theta}\dot{\psi}\left(\frac{J_y - J_z}{J_x}\right) + \frac{J_r}{J_x}\dot{\theta}\Omega + \left(c_1^2 - 1\right)e_1 - (c_1 + c_2)e_2) \\ \frac{J_y}{l}(-\dot{\phi}\dot{\psi}\left(\frac{J_z - J_x}{J_y}\right) - \frac{J_r}{J_y}\dot{\phi}\Omega + \left(c_3^2 - 1\right)e_3 - (c_3 + c_4)e_4) \\ \frac{J_x}{l}(-\dot{\phi}\dot{\theta}\left(\frac{J_y - J_z}{J_x}\right) + \left(c_5^2 - 1\right)e_5 - (c_5 + c_6)e_6) \end{bmatrix}$$

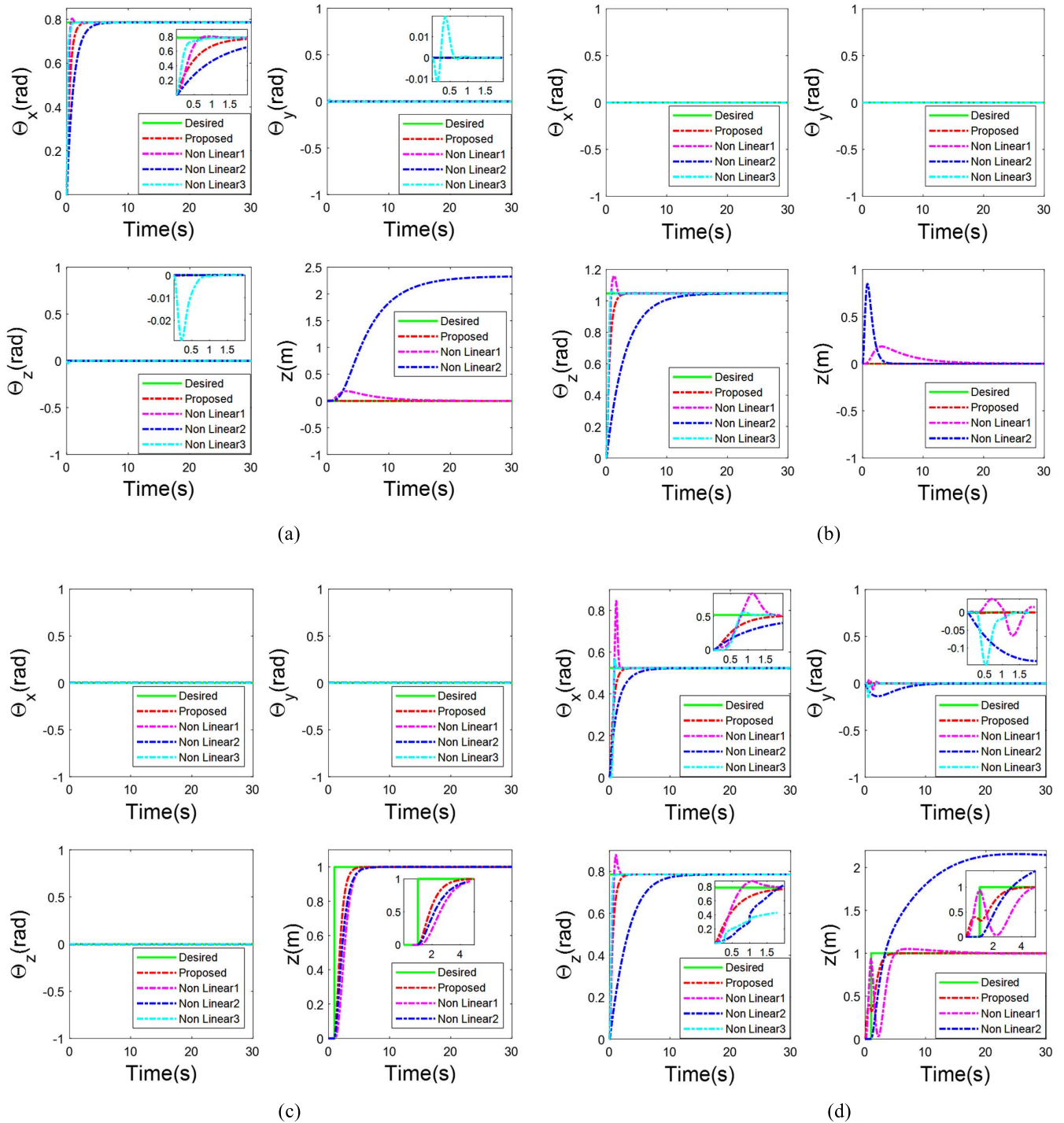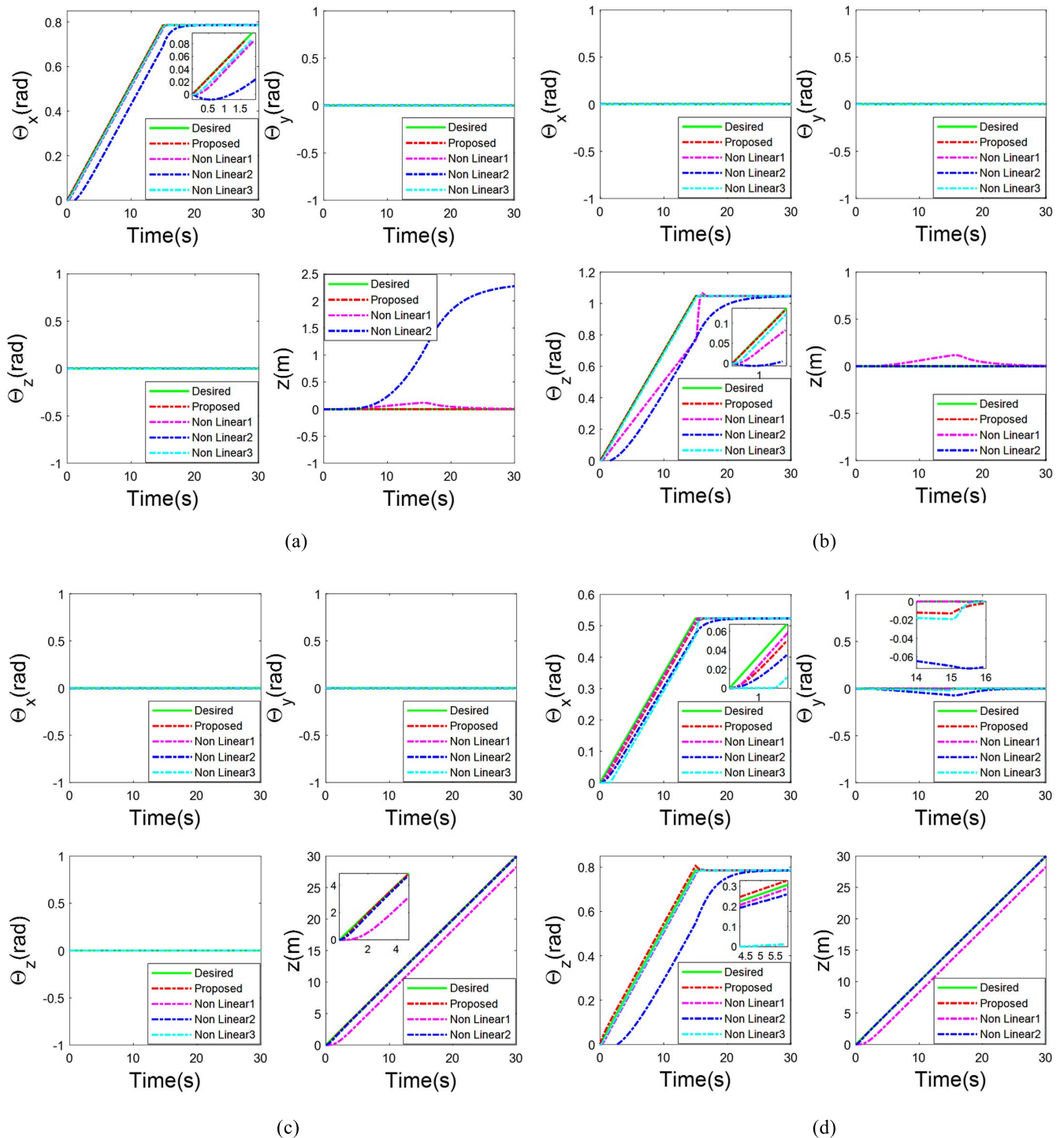$$F_b = \frac{m(g + \left(c_7^2 - 1\right)e_7 - (c_7 + c_8)e_8)}{cos\left(\phi\right)cos(\theta)}$$

FIGURE 4. Transient response of the step trajectory for the proposed system and the controllers proposed in [48], [44], and [52] (a) response to desired $\theta_{dx} = 45°$, (b) response to desired $\theta_{dz} = 60°$, (c) response to desired $z_d = 1$, and (d) response to desired $\theta_{dx} = 30°$, $\theta_{dz} = 45°$, $z_d = 1$.

bility in different states for the proposed controller and the three previous work controllers.

1) STEP TRAJECTORY

Four cases were studied: (1) response to desired $\theta_{dx} = 45°$, (2) response to desired $\theta_{dz} = 60°$, (3) response to desired $z_d = 1$, and (4) response to desired $\theta_{dx} = 30°$, $\theta_{dz} = $

$45°$, $z_d = 1$. Various quality metrics, including the steady-state error and settling time, were performed to illustrate the validity and efficiency of the proposed controller with various reference controllers. For the proposed controller, the steady-state error for the attitude and altitude in the four cases was zero. Also, the steady-state error for the three reference controllers was roughly zero with respect to

FIGURE 5. Transient response of the ramp trajectory for the proposed system and the controllers proposed in [48], [44], and [52]. (a) response to desired $\theta_{dx} = t$, from t = 0 to t = 15 s and then stabilization at $\theta_{dx} = 45°$; (b) response to desired $\theta_{dz} = t$, from t = 0 to t = 15 s and then stabilization at $\theta_{dz} = 60°$; (c) response to desired $z_d = t$; d) response to desired $\theta_{dx} = t$, $\theta_z = t$, from t=0 to t=15s, $z_d = t$ and then stabilization at $\theta_{dx} = 30°$, $\theta_z = 45°$.

the attitude response. Moreover, Nonlinear1 suffered from a noticeable overshoot. The altitude response for the two references (Non linear1, Non linear2) controllers suffered from a noticeable error as shown in Fig.4.Also, Non linear2 controller had a big error because it does not consider fric-

tion air in its controller. The settling time of the proposed system and the controllers in [48], [44], and [52], for step trajectory is presented in Table.2. Non linear3 controller showed the fastest response; however, it had a noticeable error in the transient response. Nonlinear1 and Nonlinear3
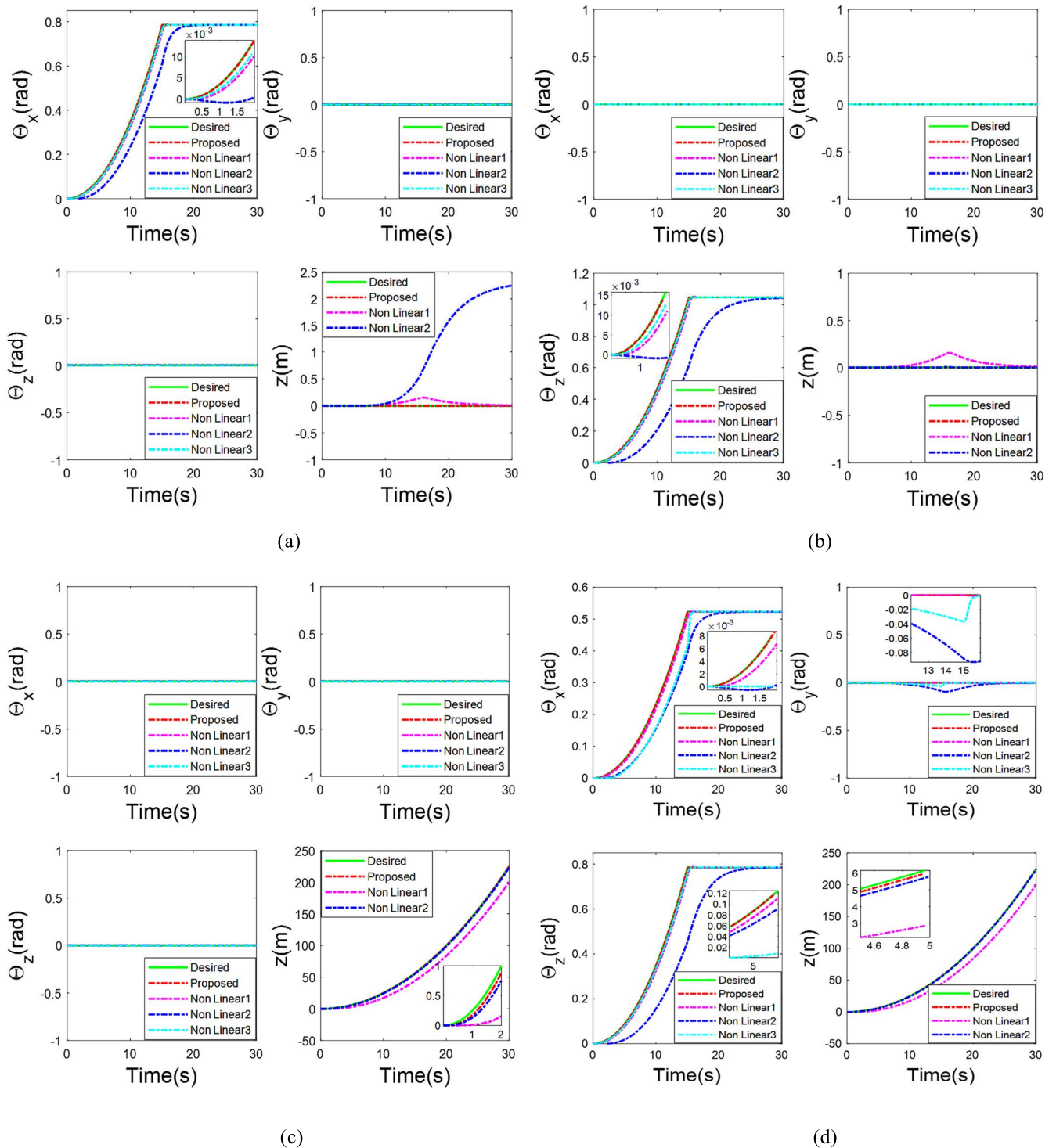
FIGURE 6. Transient response of the parabolic trajectory for the proposed system and the controllers proposed in [48], [44], and [52]. (a) response to desired $\theta_{dx} = t^2$, from t = 0 to t = 15 s and then stabilization at $\theta_{dx} = 45°$; (b) response to desired $\theta_{dz} = t^2$, from t = 0 to t = 15 s and then stabilization at $\theta_{dz} = 60°$; (c) response to desired $z_d = t^2$; (d) response to desired $\theta_{dx} = t^2$, $\theta_{dz} = t^2$, from t = 0 to t = 15s, $z_d = t^2$.

controllers showed the fastest responses with respect to the attitude response. The proposed controller was moderate with respect to the time response and the settling time for the attitude response; however, it showed the best altitude response.

TABLE 3. The Integral Absolute Error (IAE) for the proposed system and the controllers in [48], [44], and [52] for ramp trajectory.

case	Controller	Integral Absolute Error (IAE)			
		θ_x	θ_y	θ_z	Z
1	Proposed	**0.0095**	Na	Na	0
	Nonlinear1	0.0152	Na	Na	0.0418
	Nonlinear2	0.0874	Na	Na	1.9460
	Nonlinear3	0.0103	Na	Na	Na
2	Proposed	Na	Na	**0.00127**	0
	Nonlinear1	Na	Na	0.0268	~0
	Nonlinear2	Na	Na	0.2168	0
	Nonlinear3	Na	Na	0.0138	Na
3	Proposed	Na	Na	Na	**0.0025**
	Nonlinear1	Na	Na	Na	5.8467
	Nonlinear2	Na	Na	Na	0.1129
	Nonlinear3	Na	Na	Na	0
4	Proposed	0.01734	0	0.0217	**0.0025**
	Nonlinear1	**0.0101**	0	0.0178	5.9046
	Nonlinear2	0.05	0.04	0.1845	0.05
	Nonlinear3	0.0539	~0	**0.0108**	Na

TABLE 4. The Integral Absolute Error (IAE) for the proposed system and the controllers in [48], [44], and [52] for parabolic trajectory.

case	Controller	Integral Absolute Error (IAE)			
		θ_x	θ_y	θ_z	Z
1	Proposed	**~0**	Na	Na	**0**
	Nonlinear1	0.0149	Na	Na	0.0249
	Nonlinear2	0.0813	Na	Na	1.8944
	Nonlinear3	0.0101	Na	Na	Na
2	Proposed	Na	Na	**0.0012**	**0**
	Nonlinear1	Na	Na	0.0232	0.00018
	Nonlinear2	Na	Na	0.1833	~0
	Nonlinear3	Na	Na	0.0136	Na
3	Proposed	Na	Na	Na	**0.4869**
	Nonlinear1	Na	Na	Na	12.8364
	Nonlinear2	Na	Na	Na	0.6129
	Nonlinear3	Na	Na	Na	Na
4	Proposed	~0	~0	~0	**0.4869**
	Nonlinear1	0.0100	~0	0.0176	13.2029
	Nonlinear2	0.0623	0.0256	0.1339	0.6503
	Nonlinear3	0.0541	~0	0.0106	Na

2) RAMP TRAJECTORY

A saturated ramp is used instead of a normal ramp to prevent the quadcopter from spinning around itself. Four cases were studied: (1) response to desired θ_{dx} = t, from t = 0 to t = 15s and then stabilization at $\theta_{dx}45°$; (2) response to desired θ_{dz} = t, from t = 0 to t = 15s and then stabilization at θ_{dz} = 60°; (3) response to desired z_d = t; (4) response to desired θ_{dx} = t, θ_z = t, from $t = 0$ to $t = 15$s, $z_d = t$ and then stabilization at θ_{dx} = 30°, θ_z = 45°. The results of the four controllers were compared, as shown in Fig.5. For the attitude and altitude responses, the proposed controller showed the fastest response compared with the other three controllers. The integral absolute error IAE $= \frac{1}{N} \int_0^N e(t)\, dt$, was used to summarize the trajectory tracking for the ramp trajectory, as shown in Table 3. For the attitude, and the altitude response, the proposed model achieved the smallest IAE (almost zero) compared with the three reference controllers.

3) PARABOLIC TRAJECTORY

A saturated parabola is used instead of a normal parabola to prevent the quadcopter from spinning around itself. Four cases were studied: (1) response to desired $\theta_{dx} = t^2$, from t = 0 to t = 15s and then stabilization at $\theta_{dx} = 45°$; (2) response to desired $\theta_{dz} = t^2$, from t = 0 to t = 15s and then stabilization at $\theta_{dz} = 60°$; (3) response to desired $z_d = t^2$; (4) response to desired $\theta_{dx} = t^2 (\theta_{dz} = t^2$, from $t = 0$ to $t = 15s$, $z_d = t^2$) and then stabilization at $\theta_{dx} = 30°$, $\theta_z = 45°$. The four controllers were compared, as shown in Fig.6. For the attitude and altitude responses, the

proposed model showed the fastest response compared with the three reference controllers. Table 4 illustrates the IAE of trajectory tracking for parabolic trajectory. For the attitude response, the proposed model had a constant IAE (almost zero), unlike the two reference controllers. Moreover, for the altitude response, the proposed model had the lowest IAE. The Non linear2 controller had a big error in case 1.

Based on the previous results of the three trajectories, the proposed nonlinear feedback linearization tracking controller for attitude and altitude displayed accurate tracking and convergence performances compared with the three reference quadcopter controllers.

D. FLIGHT SCENARIO

Trajectory tracking performance is tested by applying various motion scenarios. Two motion scenarios were examined:

1) LINEAR SEGMENT

The quadcopter is assumed to be hovering at a height of 2m and follows a linear segment trajectory (for $t \in [0, 5]\theta_x$ change from 0 to 30°), (for $t \in [5, 10]$, $\theta_x = 30°$, θ_z change from 30° to 60°),(for $t \in [10, 15]\theta_x = 30°$, θ_y change from 30° to 45°) and (for $t > 15$, $\theta_x = 30°$, $\theta_y = 45°$, $\theta_z = 60°$). The desired attitude and altitude for the proposed controller and the three state-of-the-art controllers (Non linear1, Non linear2, Non linear3) are described in [48], [44], and [52] respectively as shown in Fig.7. The results proved the superior performance of the proposed controller compared to the comparative controllers.
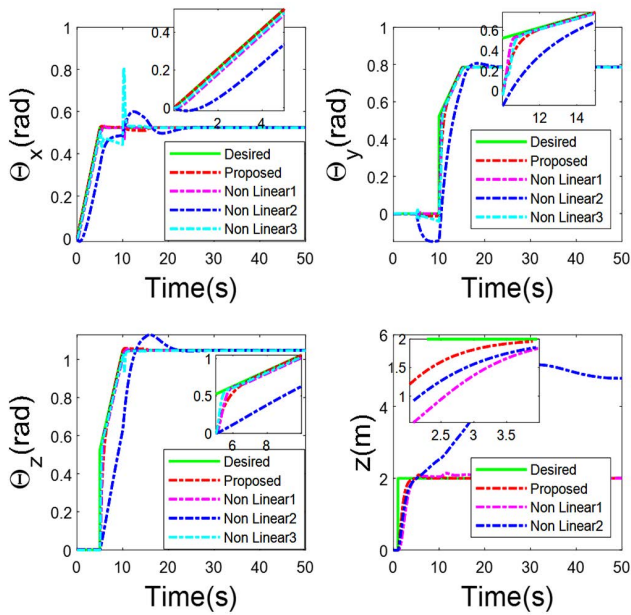
FIGURE 7. Result of flight scenario the proposed system and the controllers in [48], [44], and [52] for linear segment trajectory.
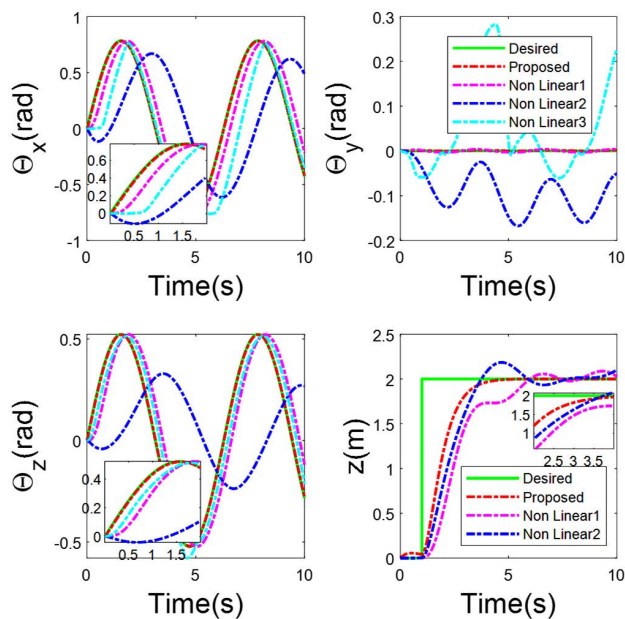

FIGURE 8. Result of flight scenario for the proposed system and the controllers in [48], [44], and [52] for sine wave trajectory.

2) SINE WAVE

The quadcopter is assumed to be hovering at a height of 2m and follows a sine wave trajectory. The desired attitude can be expressed as:

$$\theta_x = \frac{\pi}{4}\sin(t)$$
$$\theta_y = 0$$
$$\theta_z = \frac{\pi}{6}\sin(t)$$

In this flight scenario, the proposed controller also achieved the best performance in both the attitude and the altitude as shown in Fig.8.

V. CONCLUSION

In this paper, we propose a controller for tracking the attitude and altitude of quadcopter systems based on pseudo feedback linearization. The simulation results have been presented followed by comparisons between three quadcopter controllers from literature to demonstrate the proposed controller's performance. Moreover, in comparison with the reference controllers, by preserving the restrictions of the control inputs, the proposed quadcopter system can effectively track the necessary trajectories with a reasonable tracking error. As well as a quadcopter mathematical model has been developed considering the aerodynamic rotation, translation drag, and moment, which were ignored in most of the previous studies on this topic that making the controller is more realistic. The control strategy's stability was demonstrated under various trajectories (i.e., step, ramp, and parabolic trajectory) by using different metrics. The simulation presented a variety of states for the three controllers to demonstrate their stability in different states. Moreover, trajectory tracking performance is tested by applying two different flight scenarios. For both flight scenarios, the results proved the superior performance of the proposed controller compared to the comparative controllers. The Lyapunov stability theorem has been used to verify the proposed controller's global asymptotic stability.

REFERENCES

[1] Y. Naidoo, R. Stopforth, and G. Bright, "Development of an UAV for search & rescue applications: Mechatronic integration for a quadrotor helicopter," in *Proc. IEEE AFRICON Conf.*, Sep. 2011, pp. 13–15.

[2] D. Erdos, A. Erdos, and S. E. Watkins, "An experimental UAV system for search and rescue challenge," *IEEE Aerosp. Electron. Syst. Mag.*, vol. 28, no. 5, pp. 32–37, May 2013.

[3] L. Colonel, R. P. Schwing, U. States, A. Force, and P. Adviser, "Unmanned aerial vehicles—Revolutionary tools in war and peace," Army War College, Carlisle, PA, USA, Tech. Rep., Mar. 2007.

[4] M. A. Ma'sum, M. K. Arrofi, G. Jati, F. Arifin, M. N. Kurniawan, P. Mursanto, and W. Jatmiko, "Simulation of intelligent unmanned aerial vehicle (UAV) for military surveillance," in *Proc. Int. Conf. Adv. Comput. Sci. Inf. Syst. (ICACSIS)*, Sep. 2013, pp. 161–166.

[5] G. Udeanu, A. Dobrescu, and M. Oltean, "Unmanned aerial vehicle in military operations," *Sci. Res. Educ. Air Force*, vol. 18, no. 1, pp. 199–206, 2016.

[6] S. M. Meivel, A. Professor, R. Maguteeswaran, N. B. Gandhiraj, and G. Srinivasan, "Quadcopter UAV based fertilizer and pesticide spraying system," *Int. Acad. Res. J. Eng. Sci.*, vol. 1, no. 1, pp. 2414–6242, 2016.

[7] U. R. Mogili and B. B. V. L. Deepak, "Review on application of drone systems in precision agriculture," *Proc. Comput. Sci.*, vol. 133, pp. 502–509, Jul. 2018.

[8] A. K. Shastry, M. T. Bhargavapuri, M. Kothari, and S. R. Sahoo, "Quaternion based adaptive control for package delivery using variable-pitch quadrotors," in *Proc. Indian Control Conf. (ICC)*, Jan. 2018, pp. 340–345.

[9] E. G. Hernandez-Martinez, G. Fernandez-Anaya, E. D. Ferreira, J. J. Flores-Godoy, and A. Lopez-Gonzalez, "Trajectory tracking of a quadcopter UAV with optimal translational control," *IFAC-PapersOnLine*, vol. 48, no. 19, pp. 226–231, 2015.

[10] X. Zhang, X. Li, K. Wang, and Y. Lu, "A survey of modelling and identification of quadrotor robot," *Abstract Appl. Anal.*, vol. 2014, pp. 1–16, Oct. 2014.

[11] X. Wang and C. Yu, "Feedback linearization regulator with coupled attitude and translation dynamics based on unit dual quaternion," in *Proc. IEEE Int. Symp. Intell. Control*, Sep. 2010, pp. 2380–2384.

[12] C. Zha, X. Ding, Y. Yu, and X. Wang, "Quaternion-based nonlinear trajectory tracking control of a quadrotor unmanned aerial vehicle," *Chin. J. Mech. Eng.*, vol. 30, no. 1, pp. 77–92, Jan. 2017.

[13] H. Parwana, J. S. Patrikar, and M. Kothari, "A novel fully quaternion based nonlinear attitude and position controller," in *Proc. AIAA Guid., Navigat., Control Conf.*, Jan. 2018, pp. 1–12.

[14] M. Islam, M. Okasha, and E. Sulaeman, "A model predictive control (MPC) approach on unit quaternion orientation based quadrotor for trajectory tracking," *Int. J. Control, Autom. Syst.*, vol. 17, no. 11, pp. 2819–2832, Nov. 2019.

[15] C. Diao, B. Xian, B. Zhao, X. Zhang, and S. Liu, "An output feedback attitude tracking controller design for quadrotor unmanned aerial vehicles using quaternion," in *Proc. IEEE/RSJ Int. Conf. Intell. Robots Syst.*, Nov. 2013, pp. 3051–3056.

[16] B. Xian, C. Diao, B. Zhao, and Y. Zhang, "Nonlinear robust output feedback tracking control of a quadrotor UAV using quaternion representation," *Nonlinear Dyn.*, vol. 79, no. 4, pp. 2735–2752, Mar. 2015.

[17] E. Fresk and G. Nikolakopoulos, "Full quaternion based attitude control for a quadrotor," in *Proc. Eur. Control Conf. (ECC)*, Jul. 2013, pp. 3864–3869.

[18] T.-T. Tran and C. Ha, "Self-tuning proportional double derivative-like neural network controller for a quadrotor," *Int. J. Aeronaut. Space Sci.*, vol. 19, no. 4, pp. 976–985, Dec. 2018.

[19] E. Reyes-Valeria, R. Enriquez-Caldera, S. Camacho-Lara, and J. Guichard, "LQR control for a quadrotor using unit quaternions: Modeling and simulation," in *Proc. 23rd Int. Conf. Electron., Commun. Comput. (CONIELECOMP)*, Mar. 2013, pp. 172–178.

[20] K. Djamel, M. Abdellah, and A. Benallegue, "Attitude optimal backstepping controller based quaternion for a UAV," *Math. Problems Eng.*, vol. 2016, pp. 1–11, Mar. 2016.

[21] S. Gonzalez-Vazquez and J. Moreno-Valenzuela, "A new nonlinear PI/PID controller for quadrotor posture regulation," in *Proc. IEEE Electron., Robot. Automot. Mech. Conf.*, Sep. 2010, pp. 642–647.

[22] A. Alkamachi and E. Erçebi, "Modelling and genetic algorithm based-PID control of H-shaped racing quadcopter," *Arabian J. for Sci. Eng.*, vol. 42, no. 7, pp. 2777–2786, Jul. 2017.

[23] G. M. Qian, D. Pebrianti, L. Bayuaji, N. R. H. Abdullah, M. Mustafa, M. Syafrullah, and I. Riyanto, "Waypoint navigation of quad-rotor MAV using fuzzy-PID control," in *Intelligent Manufacturing & Mechatronics*. 2018, pp. 271–284, doi: 10.1007/978-981-10-8788-2_25.

[24] M. Azer and A. Ismail, "Attitude control of quadrotor using enhanced intelligent fuzzy PID controller," *Int. Res. J. Eng. Technol.*, vol. 2020, pp. 2593–2602, May 2020.

[25] I. Matei, C. Zeng, S. Chowdhury, R. Rai, and J. de Kleer, "Controlling draft interactions between quadcopter unmanned aerial vehicles with physics-aware modeling," *J. Intell. Robotic Syst.*, vol. 101, no. 1, pp. 1–21, Jan. 2021.

[26] P. De Monte and B. Lohmann, "Trajectory tracking control for a quadrotor helicopter based on backstepping using a decoupling quaternion parametrization," in *Proc. 21st Medit. Conf. Control Autom.*, Jun. 2013, pp. 507–512.

[27] X. Huo, M. Huo, and H. R. Karimi, "Attitude stabilization control of a quadrotor UAV by using backstepping approach," *Math. Problems Eng.*, vol. 2014, pp. 1–9, Feb. 2014.

[28] A. Honglei, L. Jie, W. Jian, W. Jianwen, and M. Hongxu, "Backstepping-based inverse optimal attitude control of quadrotor: Regular paper," *Int. J. Adv. Robot. Syst.*, vol. 10, pp. 1–9, May 2013.

[29] S. Zhao, W. Dong, and J. A. Farrell, "Quaternion-based trajectory tracking control of VTOL-UAVs using command filtered backstepping," in *Proc. Amer. Control Conf.*, Jun. 2013, pp. 1018–1023.

[30] S. Bouhired, M. Bouchoucha, and M. Tadjine, "Quaternion-based global attitude tracking controller for a quadrotor UAV," in *Proc. 3rd Int. Conf. Syst. Control*, Oct. 2013, pp. 933–938.

[31] M. A. M. Basri, M. S. Z. Abidin, and N. A. M. Subha, "Simulation of backstepping-based nonlinear control for quadrotor helicopter," *Appl. Model. Simul.*, vol. 2, pp. 34–40, Jul. 2018.

[32] B. Panomrattanarug, K. Higuchi, and F. Mora-Camino, "Attitude control of a quadrotor aircraft using LQR state feedback controller with full order state observer," in *Proc. SICE Annu. Conf.*, 2013, pp. 2041–2046.

[33] E. Kuantama, I. Tarca, and R. Tarca, "Feedback linearization LQR control for quadcopter position tracking," in *Proc. 5th Int. Conf. Control, Decis. Inf. Technol. (CoDIT)*, Apr. 2018, pp. 204–209.

[34] F. Muñoz, I. González-Hernández, S. Salazar, E. S. Espinoza, and R. Lozano, "Second order sliding mode controllers for altitude control of a quadrotor UAS: Real-time implementation in outdoor environments," *Neurocomputing*, vol. 233, pp. 61–71, Apr. 2017.

[35] S. Nadda and A. Swarup, "On adaptive sliding mode control for improved quadrotor tracking," *J. Vib. Control*, vol. 24, no. 14, pp. 3219–3230, 2018.

[36] H. L. N. N. Thanh and S. K. Hong, "Quadcopter robust adaptive second order sliding mode control based on PID sliding surface," *IEEE Access*, vol. 6, pp. 66850–66860, 2018.

[37] R. Akbar and N. Uchiyama, "Adaptive modified super-twisting control for a quadrotor helicopter with a nonlinear sliding surface," in *Proc. SICE Int. Symp. Control Syst. (SICE ISCS)*, Mar. 2017, pp. 1–6.

[38] D. J. Almakhles, "Robust backstepping sliding mode control for a quadrotor trajectory tracking application," *IEEE Access*, vol. 8, pp. 5515–5525, 2020.

[39] H. Bouadi and F. Mora-Camino, "Modeling and adaptive flight control for quadrotor trajectory tracking," *J. Aircr.*, vol. 55, no. 2, pp. 666–681, Mar. 2018.

[40] C. Wang, B. Song, P. Huang, and T. Tang, "Trajectory tracking control for quadrotor robot subject to payload variation and wind gust disturbance," *J. Intell. Robotic Syst.*, vol. 83, no. 2, pp. 315–333, 2016.

[41] K. Eliker, H. Bouadi, and M. Haddad, "Flight planning and guidance features for an UAV flight management computer," in *Proc. IEEE 21st Int. Conf. Emerg. Technol. Factory Autom. (ETFA)*, Sep. 2016, pp. 1–6.

[42] A. Mokhtari, N. K. M'Sirdi, K. Meghriche, and A. Belaidi, "Feedback linearization and linear observer for a quadrotor unmanned aerial vehicle," *Adv. Robot.*, vol. 20, no. 1, pp. 71–91, Jan. 2006.

[43] A. Nemati and M. Kumar, "Non-linear control of tilting-quadcopter using feedback linearization based motion control," in *Proc. ASME Dyn. Syst. Control Conf. (DSCC)*, 2014, pp. 1–8.

[44] Y.-C. Choi and H.-S. Ahn, "Nonlinear control of quadrotor for point tracking: Actual implementation and experimental tests," *IEEE/ASME Trans. Mechatronics*, vol. 20, no. 3, pp. 1179–1192, Jun. 2015.

[45] S. Stebler, W. MacKunis, and M. Reyhanoglu, "Nonlinear output feedback tracking control of a quadrotor UAV in the presence of uncertainty," in *Proc. 14th Int. Conf. Control, Autom., Robot. Vis. (ICARCV)*, Nov. 2016, pp. 13–15.

[46] A. Alkamachi and E. Erçebi, "H∞ control of an overactuated tilt rotors quadcopter," *J. Central South Univ.*, vol. 25, no. 3, pp. 586–599, Mar. 2018.

[47] M. A. Vallejo-Alarcón, M. Velasco-Villa, and R. Castro-Linares, "Robust backstepping control for highly demanding quadrotor flight," *Control Eng. Appl. Informat.*, vol. 22, no. 1, pp. 51–62, 2020.

[48] L. Martins, C. Cardeira, and P. Oliveira, "Feedback linearization with zero dynamics stabilization for quadrotor control," *J. Intell. Robotic Syst.*, vol. 101, no. 1, pp. 1–17, Jan. 2021.

[49] M. S. Esmail, M. H. Merzban, A. A. M. Khalaf, H. F. A. Hamed, and A. I. Hussein, "Attitude and altitude nonlinear control regulation of a quadcopter using quaternion representation," *IEEE Access*, vol. 10, pp. 5884–5894, 2022.

[50] M. D. Shuster, "Survey of attitude representations," *J. Astronaut. Sci.*, vol. 41, no. 4, pp. 439–517, 1993.

[51] A. Nagaty, S. Saeedi, C. Thibault, M. Seto, and H. Li, "Control and navigation framework for quadrotor helicopters," *J. Intell. Robotic Syst.*, vol. 70, nos. 1–4, pp. 1–12, Apr. 2013.

[52] A. Tayebi, "Unit quaternion-based output feedback for the attitude tracking problem," *IEEE Trans. Autom. Control*, vol. 53, no. 6, pp. 1516–1520, Jul. 2008.

[53] S. Bouabdallah, "Design and control of quadrotors with application to autonomous flying," M.S. thesis, EPFL, 2007.

MANAL S. ESMAIL received the B.Sc. degree (Hons.) from the Electrical Engineering Communications and Electronics Department, Faculty of Engineering, Fayoum University, Fayoum, Egypt, in 2012, and the M.Sc. degrees in electronics and communications engineering from Fayoum University, in 2014 and 2017, respectively. She is currently pursuing the Ph.D. degree with the Electronics and Communications Engineering Department, Faculty of Engineering, Minia University, Egypt. She has been a Lecturer Assistant with the Electronics and Communications Engineering Department, Future High institute of Engineering, Fayoum, since 2018.

MOHAMED H. MERZBAN received the B.Sc. degree from Fayoum University, the M.Sc. degree from Cairo University, and the Ph.D. degree from Egypt–Japan University for Science and Technology (E-JUST). He joined as the Teaching Staff with the Electrical Engineering Department, Faculty of Engineering, Fayoum University, Egypt, in 2006. He is currently a Lecturer with Fayoum University. His current research interests include computer vision and its applications to robotics.

ASHRAF A. M. KHALAF received the B.Sc. and M.Sc. degrees in electrical engineering from Minia University, Egypt, in 1989 and 1994, respectively, the Doctor of Engineering degree in system science and engineering from the Graduate School of Natural Science and Technology, Kanazawa University, Japan, in March 2000, and the Ph.D. degree in Egypt. He is currently a Professor of DSP and the Head of the Electronics and Communications Engineering Department, Faculty of Engineering, Minia University. His research interests include adaptive signal, audio, and image processing, AI, neural networks, machine learning, deep learning techniques, data encryption and data security, and optical communications.

HESHAM F. A. HAMED received the B.Sc. degree in electrical engineering, and the M.Sc. and Ph.D. degrees in electronics and communications engineering from Minia University, Minia, Egypt, in 1989, 1993, and 1997, respectively. He was a Professor and the Dean of the Faculty of Engineering, Minia University, till 2019. From 1989 to 1993, he worked as a Teacher Assistant with the Electrical Engineering Department, Minia University. From 1993 to 1995, he was a Visiting Scholar with Cairo University, Cairo, Egypt. From 1995 to 1997, he was a Visiting Scholar with Texas A&M University, College Station, Texas (with the group of VLSI). From 1997 to 2003, he was an Assistant Professor with the Electrical Engineering Department, Minia University. From 2003 to 2005, he was an Associate Professor with Minia University. From 2005 to 2007, he was a Visiting Researcher with Ohio University, Athens, Ohio. He is currently a Professor with the Department of Electrical Engineering, Russian University, Cairo. He has published more than 65 papers and one book chapter. His research interests include analog and mixed-mode circuit design, low voltage low power analog circuits, current mode circuits, nano-scale analog and digital integrated circuits design, and FPGA.

AZIZA I. HUSSEIN (Member, IEEE) received the B.Sc. and M.Sc. degrees from Assiut University, Egypt, in 1983 and 1989, respectively, and the Ph.D. degree in electrical and computer engineering from Kansas State University, Manhattan, KS, USA, in 2001. In 2004, she joined Effat University, Saudi Arabia, and established the first Electrical and Computer Engineering Program for women in the country and taught related courses. She was the Head of the Department of Electrical and Computer Engineering, Effat University, from 2007 to 2010. She was the Head of the Computer and Systems Engineering Department, Faculty of Engineering, Minia University, Egypt, from 2011 to 2016. She is currently the Head of the Department of Electrical and Computer Engineering, Effat University. Her research interests include microelectronics, analog/digital VLSI system design, RF circuit design, high-speed analog-to-digital converters design, and wireless communications.

● ● ●